Supporting Information

Nanoconfined ammonia borane in a flexible metal-organic framework Fe-MIL-53: clean hydrogen release with fast kinetics

Gadipelli Srinivas[a,b,]*, Will Travis[c], Jamie Ford[a,b], Hui Wu[a,d], Zheng-Xiao Guo[c] and Taner Yildirim[a,b,]*

[a]NIST Center for Neutron Research, National Institute of Standards and Technology, Gaithersburg, Maryland, 20899-6102 (USA).

[b]Department of Materials Science and Engineering, University of Pennsylbvania, Philadelphia, Pennsylvania, 19104-6272 (USA).

[c]Department of Chemistry, University College London, 20 Gordon Street, London, WC1 0AJ, (UK).

[d]Department of Materials Science and Engineering, University of Maryland, College Park Maryland, 20742-2115 (USA).

*Contact address: Fax: +1301-921-9847; Tel: +1301-975-6228; E-mail: gsrinivasphys@gmail.com (G. Srinivas); taner@seas.upenn.edu (T. Yildirim).

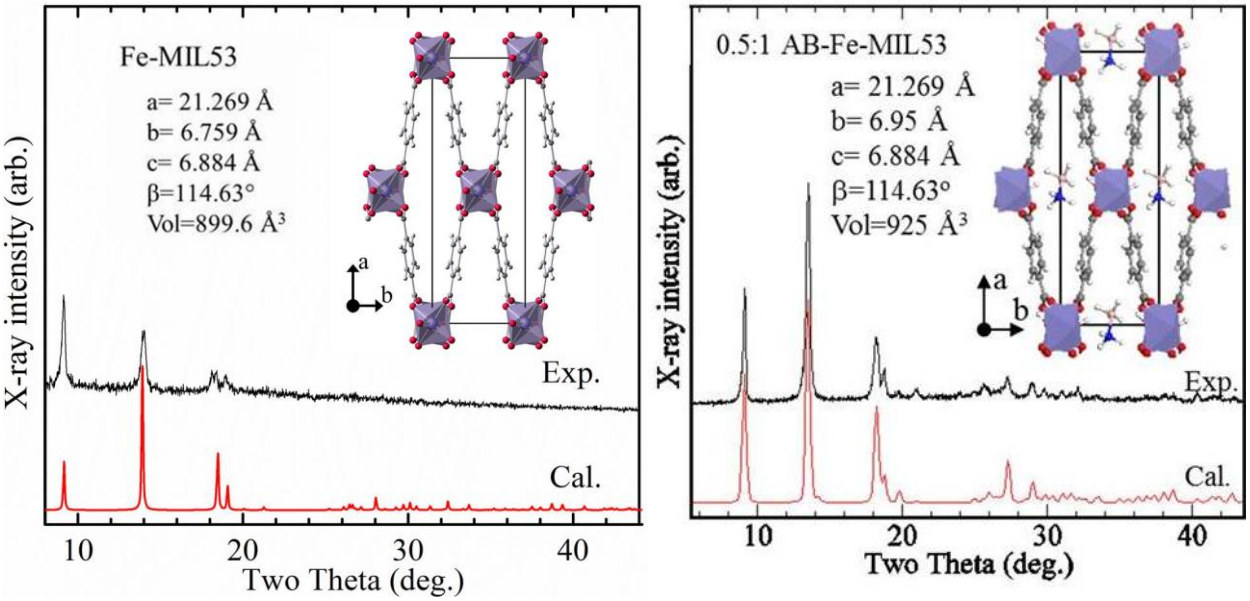

Figure S1. The measured and calculated XRD patterns of the bare Fe-MIL-53 and AB loaded Fe-MIL (0.5:1 AB:Fe). The inset shows the unit cell with very narrow pore structure and has C 2/c symmetry (gray C, red O, white H, blue B, and orange N).

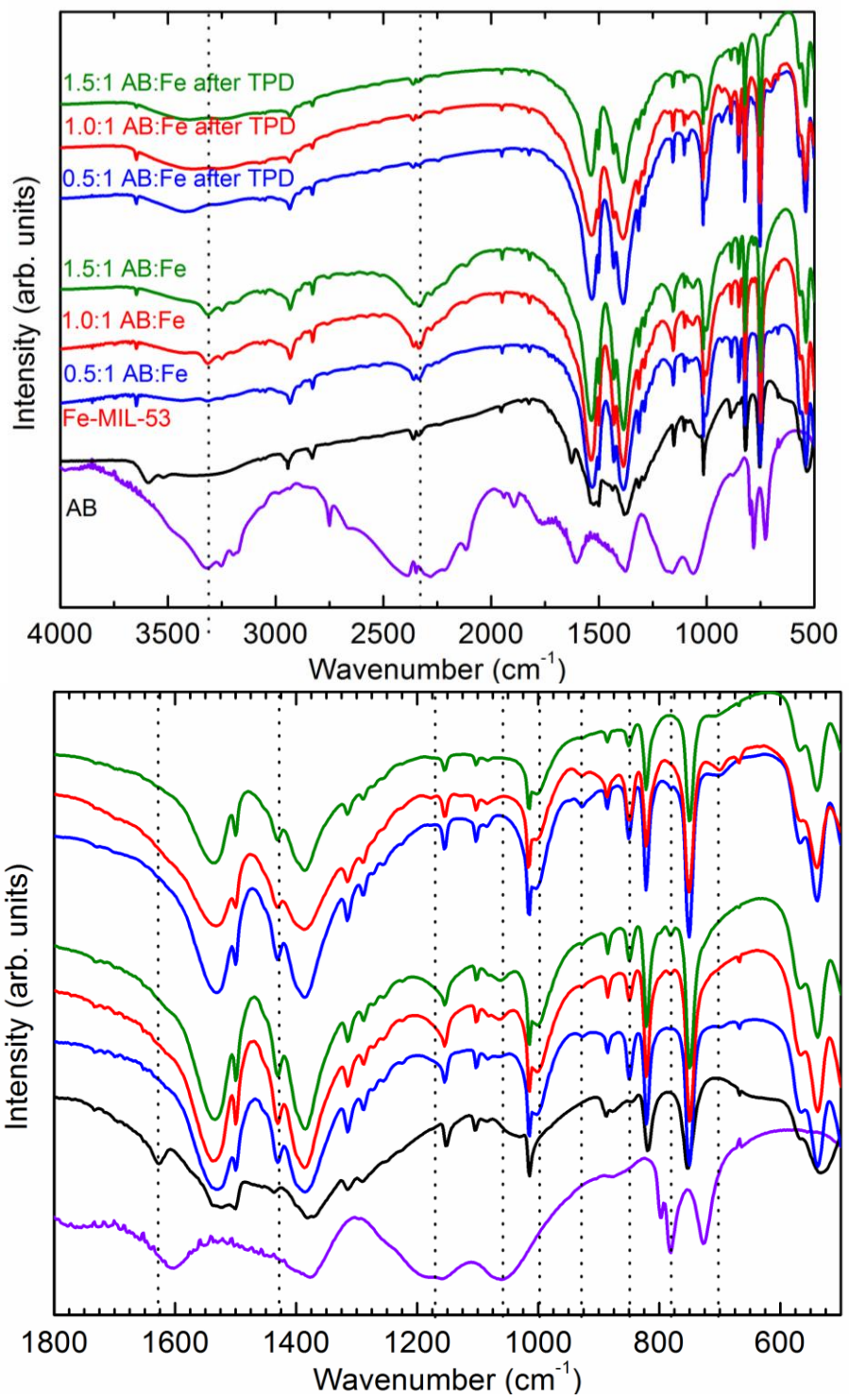

Figure S2. FTIR spectra of pristine AB, Fe-MIL-53, and AB loaded Fe-MIL-53 before and after thermal dehydrogenation. In pristine AB, the broad IR modes between 3200 cm^{-1} and 3500 cm^{-1}, and 2200 cm^{-1} and 2500 cm^{-1} correspond to the H–N and H–B stretching bonds, respectively. In addition, H–N scissor modes at 1602 cm^{-1} and 1376 cm^{-1}, H–B scissor mode at 1160 cm^{-1}, and

H- wagging modes at 1065 cm^{-1} and 727 cm^{-1} are observed. The mode at 781 cm^{-1} is assigned to B–N stretching.

The FTIR spectra of AB-MILs show combined IR modes related to the MOF and AB, but only very narrow H–N and H–B antisymmetric stretching IR modes around 3300 cm^{-1} and 2300 cm^{-1} respectively, is seen in infiltrated AB. This explains the significantly reduced AB–AB intermolecular interactions in the infiltrated AB molecules. After TPD run, the IR modes of H–N stretching bonds are seen at around 3400 cm^{-1}, however the H–B IR modes have disappeared, normally appear at around 2500 cm^{-1} in AB after 200 ^{o}C thermolysis. It is worth noticing that there are additional new IR modes at ~1010 cm^{-1}, ~925 cm^{-1}, 850 cm^{-1}, ~696 cm^{-1}, in AB-Fe-MIL before and after thermal desorption. The –OH vibration at ~1630 cm^{-1} in the MOF has disappeared in AB loaded MOFs. These are assigned to the coordination of B with oxygen functional groups in MOF pores **[I. Markova-Deneva, Infrared spectroscopy investigation of metallic nanoparticles based on copper, cobalt, and nickel synthesized through borohydride reduction method (review).** ***Journal of the University of Chemical Technology and Metallurgy, 45, 4, 2010, 351-378*****].** The B coordination with oxygen functional groups is also seen earlier in other AB loaded MOFs (AB-Mg-MOF-74 and AB-Zn-MOF-74) **[S. Gadipelli, J. Ford, W. Zhou, H. Wu, T. J. Udovic and T. Yildirim, Nanoconfinement and catalytic dehydrogenation of ammonia borane by magnesium-metal-organic framework-74,** ***Chem. Eur. J.*****, 2011, 17, 6043-6047. G. Srinivas, J. Ford, W. Zhou and T. Yildirim, Zn-MOF assisted dehydrogenation of ammonia borane: enhanced kinetics and clean hydrogen generation** ***Int. J. Hydrogen Energy*****, 2011, 37, 3633-3638.].**

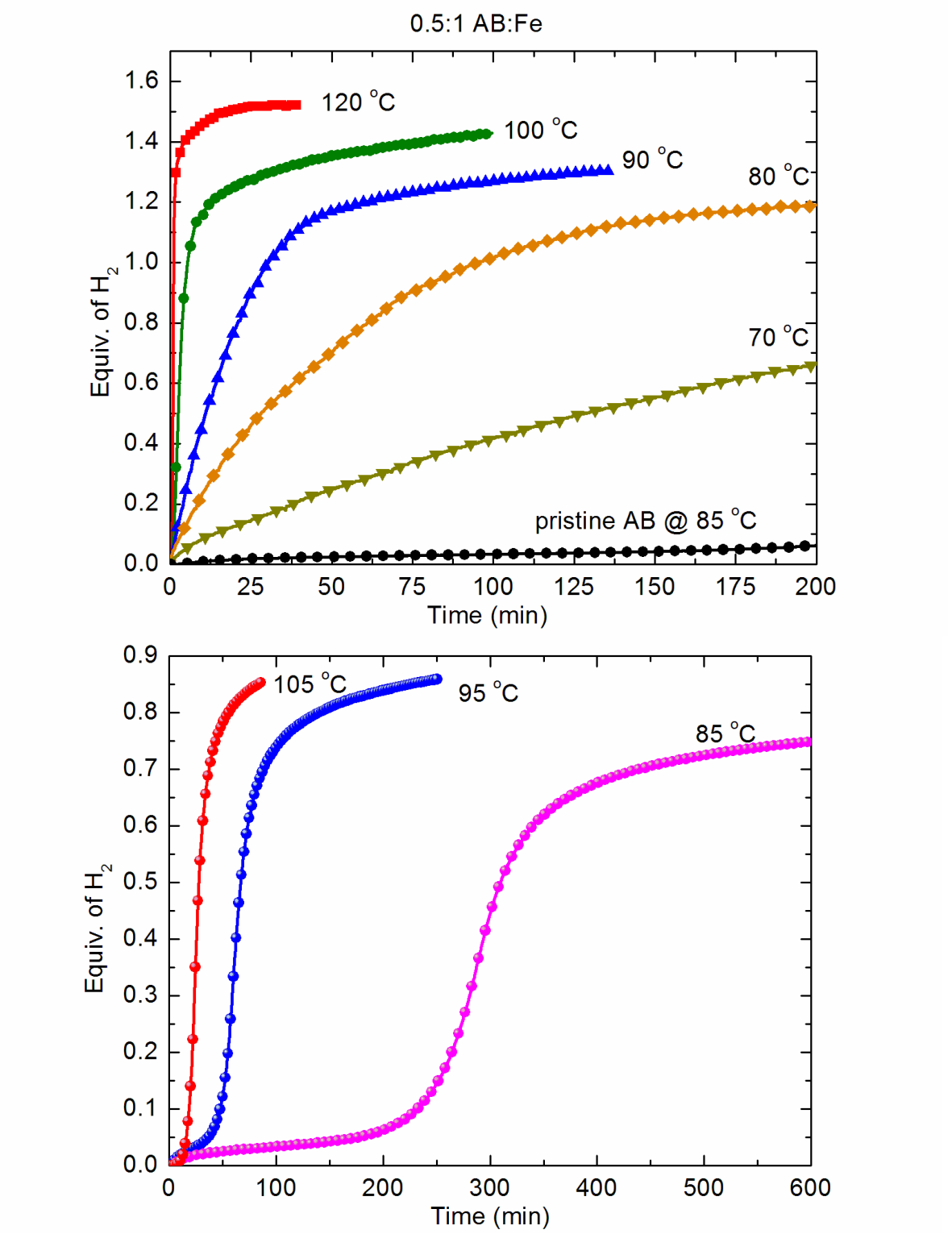

Figure S3. Isothermal hydrogen desorption kinetics at different constant temperatures of pristine AB and AB loaded Fe-MIL-53 with 0.5:1 AB:Fe.

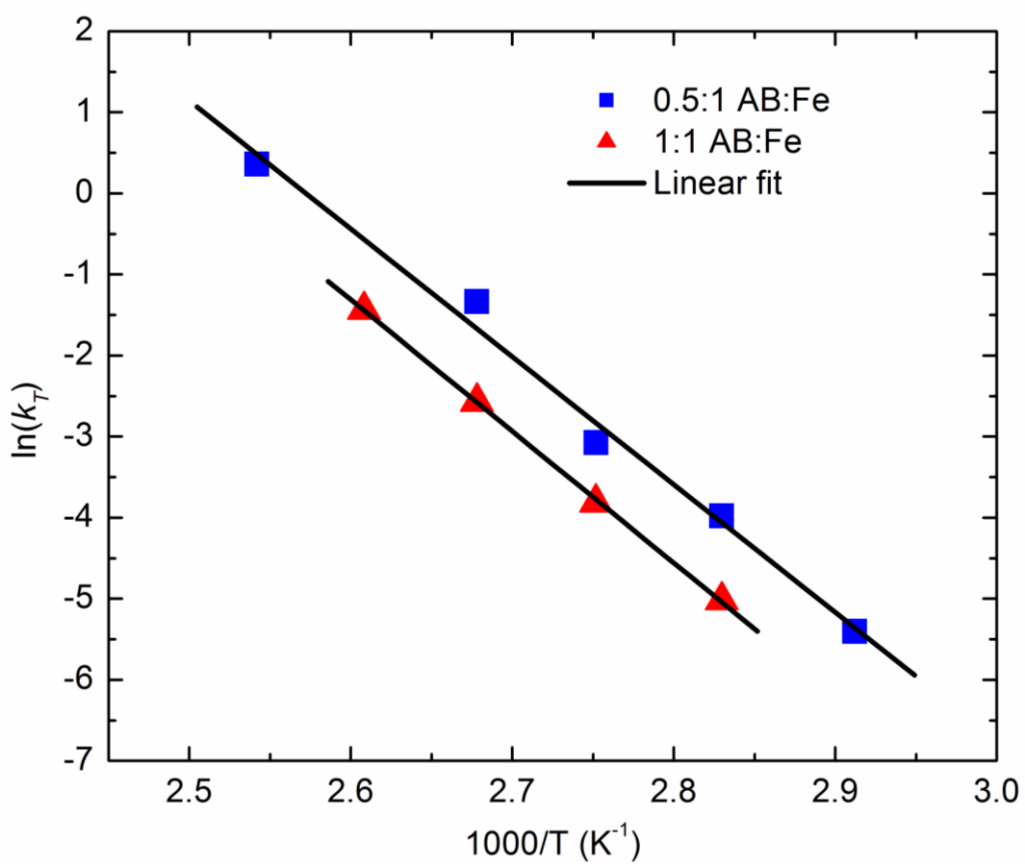

Figure S4. Arrhenius plots of the dehydrogenation kinetics of the AB-Fe-MIL-53 with 0.5:1 AB:Fe and 1:1 AB:Fe

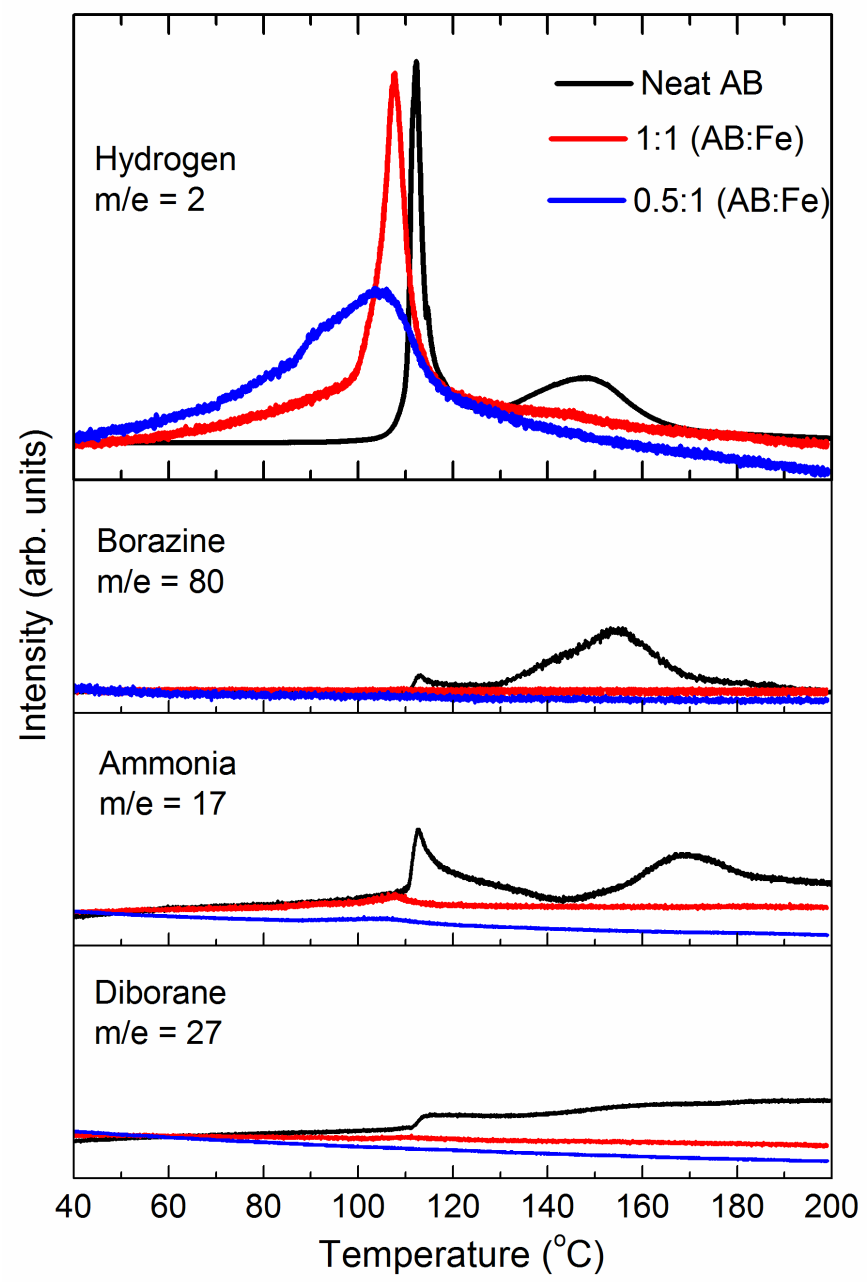

Figure S5. The mass spectroscopy data showing the clean hydrogen release from nanoconfined AB in Fe-MIL pores, whereas in pristine AB along with hydrogen the release of byproducts of ammonia, borazine and diborane is seen.

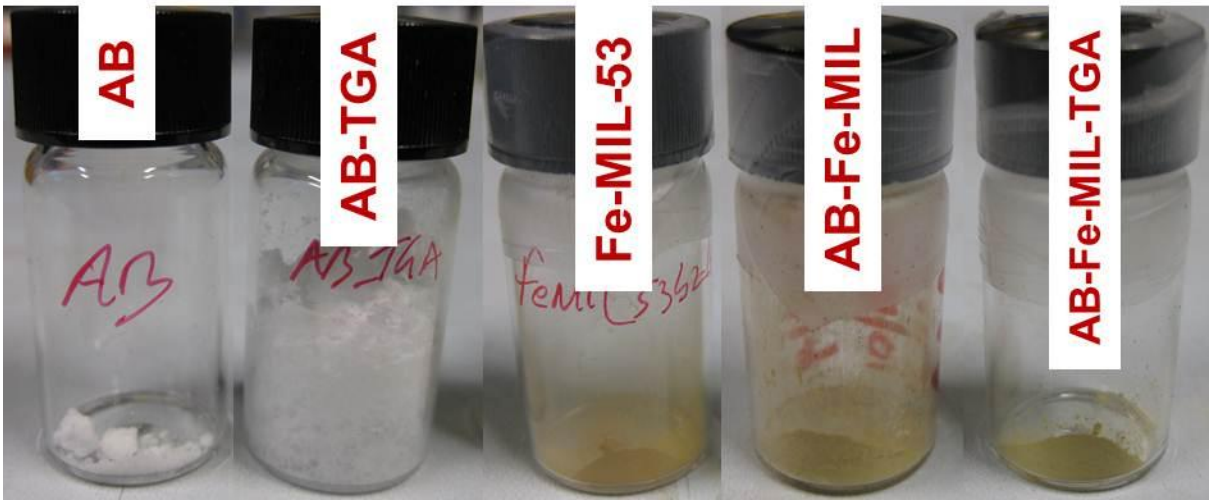

Figure S6. Photographs of pristine AB and Fe-MIL-53, and AB-Fe-MIL (1:1 AB:Fe) samples before and after thermal dehydrogenation (TGA) shows the extensive sample foaming is suppressed in nanoconfined AB sample.

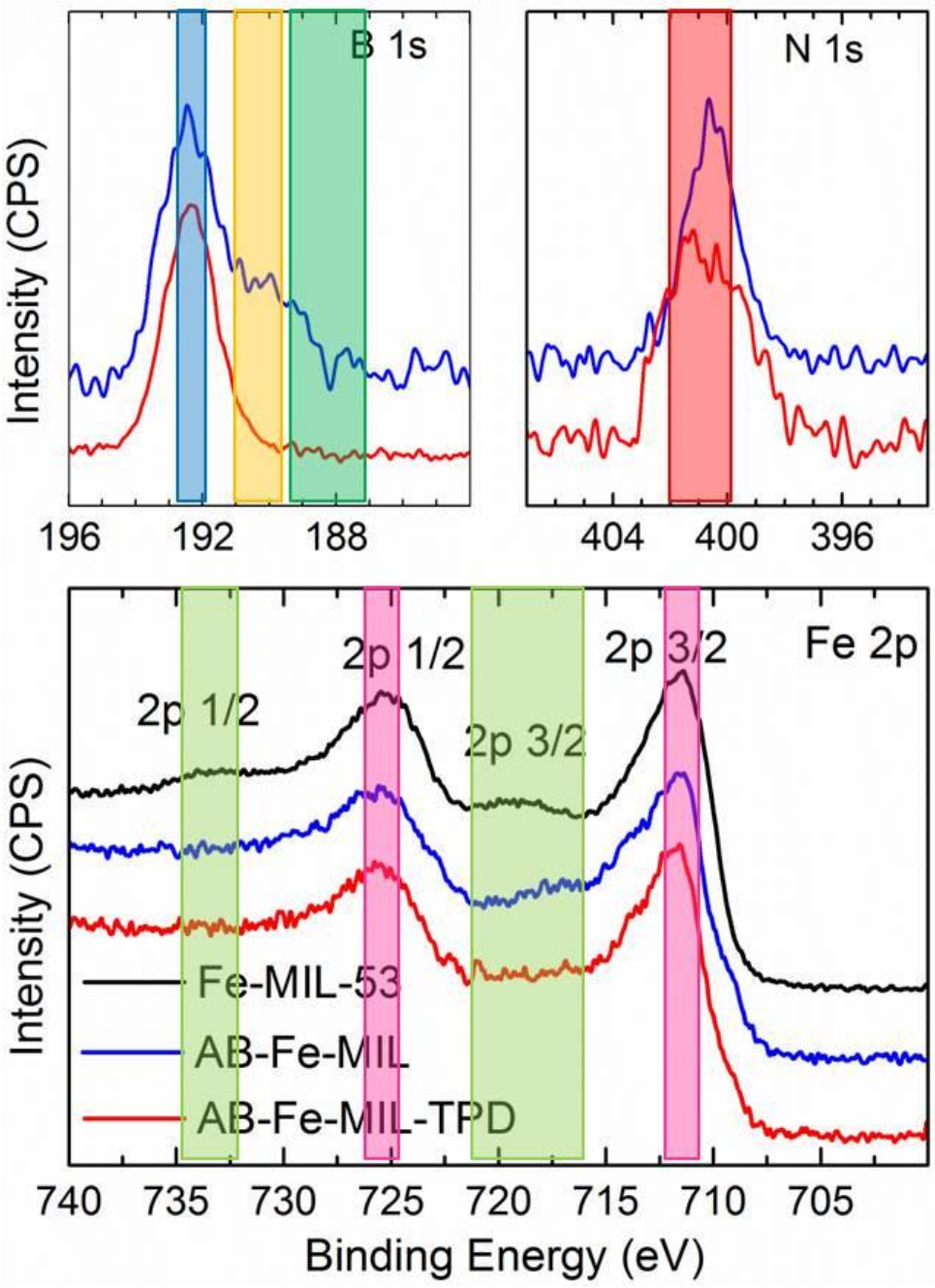

Figure S7. XPS B1s, N 1s, and Fe 2p core level spectra of Fe-MIL-53 and AB-Fe-MIL (1:1 AB:Fe) samples before and after thermal dehydrogenation at 200 ^{o}C.

In B 1s XPS core level spectra the BE of ~192.0 eV and ~188 eV are assigned to B–O and B–H bonds, respectively. The peak around 190 eV is assigned to B–N bonds, implying that not all the B–N bonds are broken in AB-Fe-MIL before thermal desorption [**J. Zhao, J. Shi, X. Zhang, F. Cheng, J. Liang, Z. Tao and J. Chen, A soft hydrogen storage material: poly(methyl acrylate)-confined ammonia borane with controllable dehydrogenation, Adv. Mater. 2010,**

22, 394–397.]. The B 1s and N 1s peaks in AB-Fe-MIL before and after thermal desorption also show no evidence of poly-(aminoborane) with binding energies of 191.1 eV for B 1s and 398.2 eV for N 1s or the counterpart boron nitride with 190.2 eV for B 1s and 397.9 eV for N 1s [R. A. Geanangel and J. W. Rabalais, **Evidence from mass spectra and X-ray photoelectron spectra concerning the structure of poly(aminoborane),** ***Inorganica Chimica Acta*****, 1985, 97, 59-64].** The broad N 1s peak between 403 eV and 398 eV (centered between 401 eV and 402 eV) in AB-Fe-MIL-TPD sample is assigned to $–NH_2–$Fe and $–NH_2–$O bonds [**Y. Wang, B. Li, Y. Zhou, D. Jia and Y. Song, CS-Fe(II,III) complex as precursor for magnetite nanocrystal,** ***Polym. Adv. Technol.*****, 2011, 22, 1681–1684]**. Fe 2p peaks of Fe-MIL-53 at BE ~711 eV and ~725 eV are assigned to Fe $2p_{3/2}$ and Fe $2p_{1/2}$ for iron(III) oxide, the additional satellite peaks at ~718 eV and ~730 eV are associated with Fe $2p_{3/2}$ and Fe $2p_{1/2}$, the spectra clearly resembles the Fe_2O_3 standard sample. The AB-Fe-MIL before and after thermal desorption exhibits similar spectra but with a shifted Fe $2p_{3/2}$ satellite peak to lower BE (~716 eV in AB-Fe-MIL) or no satellite peaks (in AB-Fe-MIL-TPD), respectively. It has been previously reported that Fe $2p_{3/2}$ for Fe_3O_4 ($FeO.Fe_2O_3$ with Fe(II).Fe(III)) does not have a satellite peak. In case of $Fe_{1-y}O$, the satellite peak for Fe $2p_{3/2}$ was observed at 715.5 eV [**T. Yamashita, P. Hayes, Analysis of XPS spectra of Fe^{2+} and Fe^{3+} ions in oxide materials,** ***Appl. Surf. Sci.*****, 2008, 254, 2441–2449.**].

First-Principles Calculations

In order to determine the hydrogen positions as well as the AB-molecule orientation and its location in MIL, we have performed first-principles structural optimization using Quantum Espresso Code PWSCF [P. Giannozzi et. al, J. Phys. Condens. Matter, 21, 395502 (2009)]. We used Vanderbilt-type ultrasoft pseudopotentials and the generalized gradient approximation (GGA) with the Perdew-Burke-Ernzerhof (PBE) exchange correlation. A kinetic energy cutoff of 544 eV and a *k*-point sampling with dk=0.03 $Å^{-1}$ grid spacing were found to be enough for the total energy to converge within 0.5 meV/atom. AB molecules were introduced to the center of MIL structure assuming various initial orientations, followed by full atomic structural relaxation. The lattice parameters are kept constant at the experimental values but all the atomic positions are optimized until the maximum force is 0.005 eV/Ang. Below we list the optimized atomic positions for 0.5:1 loaded Fe-MIL. The simulated x-ray patterns shown in the text were obtained from these optimized atomic positions.

0.5:1 AB-Fe-MIL-53 Lattice Parameters and Optimized Atomic Positions

Cell: 21.2690 6.8839 6.9499 90.0000 114.6300 90.0000
ATOMIC_POSITIONS (crystal)
O 0.449176561 0.302978213 0.314712366
O 0.574583529 0.316060869 0.165448578

O	0.577091907	0.692695802	0.663903747
O	0.442258605	0.680144216	0.803812701
O	0.949170611	0.803056914	0.315249349
O	0.074719260	0.816387815	0.165617781
O	0.077123353	0.192807887	0.664017872
O	0.942119395	0.179984162	0.804111061
O	0.428209840	0.382435190	0.975869197
O	0.592483567	0.354296406	0.513093376
O	0.594819815	0.650856832	0.009924017
O	0.424296850	0.627861526	0.460233073
O	0.928266909	0.882069210	-0.023656119
O	0.092577062	0.854452556	0.513249088
O	0.094828620	0.151012623	0.010002310
O	0.924307203	0.128134094	0.460553502
O	1.012681950	0.893715445	0.745130216
O	1.013434427	0.129240470	0.245074787
O	0.512681709	0.393490392	0.744966516
O	0.513414824	0.629227833	0.244826761
C	0.334462678	0.268105248	0.044952018
C	0.685013612	0.246445770	0.431261393
C	0.691388954	0.716220551	0.928350311
C	0.326925666	0.682722786	0.543071407
C	0.834474939	0.767842429	0.045322997
C	0.185147297	0.746778415	0.431399537
C	0.191415818	0.216211977	0.928300442
C	0.826838043	0.182882292	0.543075357
C	0.308769650	0.236140250	0.198395672
C	0.709098546	0.206189127	0.275010745
C	0.717240933	0.742938126	0.773378498
C	0.302758631	0.717989592	0.699933437
C	0.808722491	0.735967218	0.198660186
C	0.209202533	0.706345608	0.275094139
C	0.217210181	0.243127543	0.773216146
C	0.802616548	0.217854878	0.699887513
C	0.238441513	0.209360428	0.141684556
C	0.779167626	0.174804951	0.330159458
C	0.787821893	0.767257951	0.830526812
C	0.232765133	0.749654589	0.644988596
C	0.738369112	0.709437481	0.141789633
C	0.279253449	0.674681775	0.330204233
C	0.287782163	0.267510972	0.830225859
C	0.732600145	0.249224809	0.644851085
C	0.409465141	0.319994653	0.115265677
C	0.611356827	0.308677312	0.365627361
C	0.615759118	0.683557045	0.864785469

C	0.403240595	0.659644783	0.606529464
C	0.909487314	0.819775218	0.115729189
C	0.111482098	0.808979206	0.365813318
C	0.115787493	0.183603741	0.864896793
C	0.903177949	0.159802489	0.606729526
H	0.344559968	0.234795777	0.364400042
H	0.672220910	0.205247596	0.109276173
H	0.681181218	0.744009520	0.606884016
H	0.340178815	0.726027167	0.864613102
H	0.844484180	0.734374637	0.364681653
H	0.172331556	0.705538666	0.109385049
H	0.181134928	0.244285559	0.606750553
H	0.839994328	0.225797766	0.864597417
H	0.219437268	0.184449516	0.263012478
H	0.797805394	0.148689849	0.208304331
H	0.807228596	0.787994053	0.709608842
H	0.214572257	0.782350980	0.766682586
H	0.719325651	0.684809071	0.263085788
H	0.297885994	0.648433818	0.208336225
H	0.307164704	0.288338732	0.709258748
H	0.714367078	0.281491441	0.766568749
H	0.468453906	0.312901130	0.698534505
H	0.542428685	0.745734802	0.285949504
H	0.968467030	0.813075401	0.698740602
H	1.042315793	0.246018949	0.286000679
H	0.532085141	0.090114889	0.728200257
H	0.437575291	1.031300055	0.862300473
H	0.500456786	0.872214405	0.637597878
H	0.408189835	0.237385099	0.638287586
H	0.478783959	0.065748811	0.477499825
H	0.374055367	0.983254198	0.554384945
H	0.032322019	0.590031013	0.729940483
H	0.937397358	0.530970511	0.862100769
H	0.000667893	0.372502596	0.637856473
H	0.908229141	0.737341229	0.638542389
H	-0.020754225	0.566860667	0.478855108
H	0.874273733	0.483133736	0.553849398
Fe	0.011796885	0.011845284	-0.007141601
Fe	1.011288915	0.002714805	0.489644268
Fe	0.511800338	0.511769911	-0.007347468
Fe	0.511267235	0.502557561	0.489396879
N	0.488490868	0.017421540	0.627751355
N	-0.011238667	0.517744897	0.628692102
B	0.423992104	1.066203532	0.679716094
B	0.924071674	0.566153160	0.679774739